Numerical Experiments with Self-Adaptive Finite Element Simulations in 2D for the Carbonation of Concrete

Alfred Schmidt, Adrian Muntean, and Michael Böhm

Zentrum für Technomathematik, FB 3, Universität Bremen, 28334 Bremen, Germany

Abstract

Chemical processes like carbonation of concrete structures are driven by slow diffusion processes and fast reactions. This leads to the formation of relatively sharp reaction fronts, which move slowly through the material. Self-adaptive finite element methods provide a tool to automatically generate meshes locally fine enough to capture the reaction, while coarser meshes are sufficient in the bulk. We demonstrate here the applicability of self-adaptive methods for 2D concrete carbonation problems.

Key words: Adaptive finite element method, reaction-diffusion systems, concrete carbonation, fast reaction

1 Introduction: Need for automatic adaptivity

During carbonation of concrete structures and similar physicochemical processes, relatively sharp reaction fronts move slowly through the material, driven by diffusion processes. In other parts, concentration fields vary only slightly (or not at all).

In order to capture such reaction fronts in a numerical method, a high resolution (equivalent to a fine grid) is needed in those places. But using such a fine grid everywhere, the computation will get very slow, especially in two and three space dimensions. The reason is the stiffness of equations due to high reaction rates, which require stable (and expensive) numerical solution methods and relatively small time steps. On the other hand, such a fine grid is not needed everywhere, because slowly varying concentration fields can easily be approximated on a relatively coarse mesh. Thus, a method which uses a fine mesh near reaction fronts and coarser meshes where possible would make a good balance between accuracy and numerical cost.

Adaptive finite element methods present a tool to automatically give criteria for a local mesh refinement, based on the computed solution (and not only on *a priori* knowledge of an expected behavior). For model problems, even mathematical bounds for the error between approximate and true solution can be shown, as well as quasi-optimality of the meshes generated by the adaptive method. In self-adaptive methods, regions for local refinement

are selected based on local error indicators, which estimate the error contribution of single mesh elements. They are computed from the discrete solution on the current mesh and known data of the problem (like material parameters and boundary values). All mesh elements where these indicators are large must be refined, while elements with very small indicators may even be coarsened. This is important especially for simulations of non-stationary problems, when local internal structures may move or even vanish after some time.

We want to demonstrate here that is is appropriate to apply such self-adaptive finite element methods to a model for the carbonation of concrete in two space dimensions. In the moment, this is only a test for this application, as mathematical proofs for error bounds are not yet derived, and thus error indicators are still purely heuristical. Due to the strong reaction and slow diffusion, it is not even clear what is an appropriate error norm to work with – using the standard L^2-norm based derivation of adaptive methods would need a Gronwall-like estimate, introducing exponentials of the reaction rate and time scale, which are both large, and thus produce practically irrelevant estimates.

For a survey of durability problems in concrete-based materials, see [5], e.g., and references therein. Specifics on concrete carbonation are subject of [2, 11]. First attempts to deal with 2D carbonation issues (under natural exposure conditions of concrete structures) are published in [1, 7, 10].

2 Concrete carbonation model

For demonstration purposes, we restrict ourselves here to a simple reaction-diffusion model in 2D for the carbonation of concrete, involving the concentrations c_1, c_2 of CO_2 in air and liquid phases, c_3 of $Ca(OH)_2$ in water, and the total moisture concentration c_4. In a domain $\Omega \subset \mathbb{R}^2$, the carbonation can be modeled by the system of reaction-diffusion equations

$$\begin{aligned}
\partial_t c_1 - D_1 \Delta c_1 &= -f^{\text{Henry}}, && (1)\\
\partial_t c_2 - D_2 \Delta c_2 &= f^{\text{Henry}} - f_2^{\text{reac}}, && (2)\\
\partial_t c_3 - D_3 \Delta c_3 &= -f_3^{\text{reac}}, && (3)\\
\partial_t c_4 - D_4 \Delta c_4 &= f_4^{\text{reac}}. && (4)
\end{aligned}$$

Absorption of CO_2 from gaseous to water phase is described by f^{Henry}, while f_i^{reac} denote the productions of species i by the carbonation reaction. This system of equations is completed by appropriate initial values and flux boundary conditions. See [6] for a derivation of this and similar models.

Moving to non-dimensional concentrations $u_i = c_i/c_i^m$ and characteristic time/length scales (compare [6], e.g.), integrating over Ω with a test function v, and integrating the Laplacian by parts, this leads to the weak formulation of (1)-(4) in the Sobolev space $H^1(\Omega)$: For all $v \in H^1(\Omega)$ and times $t \in (0, T)$ holds

$$(\partial_t u_1, v)_\Omega + \quad \delta_1 (\nabla u_1, \nabla v)_\Omega = (-f^{\text{Henry}}, v)_\Omega + W_1^{\text{Rob}} (u_1^{\text{ext}} - u_1, v)_{\partial\Omega}, \qquad (5)$$

$$\beta_2(\partial_t u_2, v)_\Omega + \beta_2\delta_2(\nabla u_2, \nabla v)_\Omega = (f^{\text{Henry}} - f^{\text{reac}}, v)_\Omega, \quad (6)$$
$$\beta_3(\partial_t u_3, v)_\Omega + \beta_3\delta_3(\nabla u_3, \nabla v)_\Omega = (-f^{\text{reac}}, v)_\Omega, \quad (7)$$
$$\beta_4(\partial_t u_4, v)_\Omega + \beta_4\delta_4(\nabla u_4, \nabla v)_\Omega = (f^{\text{reac}}, v)_\Omega + W_4^{\text{Rob}}(u_4^{\text{ext}} - u_4, v)_{\partial\Omega}. \quad (8)$$

Here, $(v, w)_G := \int_G vw$ denotes the L^2-scalar product, and u_i^{ext} is the exterior value giving the flux boundary condition with mass transfer coefficient W_i^{Rob}, which is used here only for gaseous CO_2 and moisture. The system is completed by initial values for $u_1, \ldots, u_4$ at time $t = 0$. They account for the cement chemistry. The absorption and reaction production terms are given by

$$f^{\text{Henry}} = W^{\text{Hen}}\Big(\frac{C^{\text{Hen}}u_1}{\phi\phi_a} - \frac{\beta_2 u_2}{\phi\phi_w}\Big), \quad f^{\text{reac}} = \Phi^2 F^{\text{Hum}} \frac{u_2^p u_3^q}{(\phi\phi_w)^{p+q-1}},$$

where we denote by ϕ the concrete porosity, ϕ_a, ϕ_w air and water fractions in pores, C^{Hen} the Henry constant, W^{Hen} is an absorption constant, and F^{Hum} is a (constant) humidity factor. The exponents $p, q \geq 1$ are partial reaction orders of the carbonation reaction. Due to the scaling, the previously different reaction production terms now are all the same. The β_i are called impact capacity factors and represent the ratio of the maximum concentration of the i-th species to the maximum $CO_2(g)$ concentration. We denote by δ_i the ratio of the characteristic diffusion time of the $CO_2(g)$ to the characteristic diffusion time of the i-th species. The ratio of the characteristic time for diffusion to the characteristic time for reaction gives the dimensionless coefficient Φ^2, the Thiele modulus.

3 Finite element approximation

Based on the weak formulation (5)-(8), we derive a finite element method by time discretization and looking for solutions in each time step in a finite dimensional subspace of $H^1(\Omega)$.

Let $0 = t_0 < t_1 < \ldots < t_N = T$ define a subdivision of $(0, T)$ into time steps $I_n = (t_{n-1}, t_n)$ with (not necessarily constant) time step sizes $\tau_n = t_n - t_{n-1}$. For each time step, let $\mathcal{S}_n$ be a conforming triangulation of Ω into triangles. Here we assume that the domain has polygonal boundary $\partial\Omega$. Corresponding to these triangulations, we define the spaces X_n of piecewise linear finite element functions $X_n = \{v \in C(\bar{\Omega}) : v|_S \in \mathbb{P}_1(S) \text{ for all } S \in \mathcal{S}_n\}$.

Using an implicit Euler time discretization, we define in every time step the discrete solution $U_1^n, U_2^n, U_3^n, U_4^n \in X_n$, fulfilling for each $V \in X_n$

$$(\frac{U_1^n - U_1^{n-1}}{\tau_n}, V)_n + \quad \delta_1(\nabla U_1^n, \nabla V)_\Omega = (-f^{\text{Henry}}, V)_n + W_1^{\text{Rob}}(u_1^{\text{ext}} - U_1^n, V)_{\partial\Omega}, \quad (9)$$
$$\beta_2(\frac{U_2^n - U_2^{n-1}}{\tau_n}, V)_n + \beta_2\delta_2(\nabla U_2^n, \nabla V)_\Omega = (f^{\text{Henry}} - f^{\text{reac}}, V)_n, \quad (10)$$
$$\beta_3(\frac{U_3^n - U_3^{n-1}}{\tau_n}, V)_n + \beta_3\delta_3(\nabla U_3^n, \nabla V)_\Omega = (-f^{\text{reac}}, V)_n, \quad (11)$$

$$\beta_4(\frac{U_4^n - U_4^{n-1}}{\tau_n}, V)_n + \beta_4\delta_4(\nabla U_4^n, \nabla V)_\Omega \;=\; (f^{\rm reac}, V)_n + W_4^{\rm Rob}(u_4^{\rm ext} - U_4^n, V)_{\partial\Omega}. \quad (12)$$

Here, $(V,W)_n := \int_\Omega I_n(VW)$ denotes the *lumped* L^2-scalar product, where I_n is the Lagrange interpolation operator. Using this scalar product (which is equivalent to a quadrature formula using only values in vertices), the mass matrix $[(V_i,V_j)_n]$ reduces to a diagonal matrix, where $\{V_i, i = 1,\ldots,dim(X_n)\}$ denotes the Lagrange basis of X_n. Especially, this decouples the nonlinear reaction functions in each vertex of the triangulation, making the solution easier to compute. Additionally, mass lumping leads to a discrete maximum principle (when the triangulation is weakly acute), and thus prevents a possible overshooting of the solution. This system of nonlinear equations is solved in each time step by a modified Newton method.

Different meshes $\mathcal{S}_n$ will be used in each time step, with local mesh size controlled automatically by the adaptive method described next.

4 Error indicators and adaptive method

The usual derivation of error estimates for finite element discretization of (linear and weakly nonlinear) parabolic problems

$$\dot u - \Delta u + f(u) = 0 \;\text{ in } \Omega, \quad \nu\cdot\nabla u = g \;\text{ on } \partial\Omega, \quad u(\cdot,0) = u_0$$

leads to error estimates (compare [3, 4, 8]) like

$$\max_{1\le n\le N} \|u(t_n) - U^n\|_\Omega \;\le\; \Big(\sum_{S\in\mathcal{S}_0}(\eta_{0,S})^2\Big)^{\frac12} + \max_{1\le n\le N}\left(\eta_{n,\tau} + \Big(\sum_{S\in\mathcal{S}_n}(\eta\eta_{n,S})^2\Big)^{\frac12}\right),$$

where $\eta_{0,S}, \eta_{n,\tau}, \eta_{n,S}$ are *computable* error indicators depending only on the discrete solution and known data of the problem,

$$\begin{aligned}
(\eta_{0,S})^2 &= \|u_0 - U^0\|_S^2, \quad S\in\mathcal{S}_0,\\
\eta_{n,\tau} &= C_\tau\|U^n - U^{n-1}\|_\Omega,\\
(\eta_{n,S})^2 &= C_h\Big(h_S^4\Big\|\frac{U^n - I_nU^{n-1}}{\tau_n} - \Delta U^n + f(U^n)\Big\|_S^2\\
&\qquad + \sum_{\Gamma\subset\partial S\cap\Omega} h_S^3\,\|[\nabla U^n]_\Gamma\|_\Gamma^2 \;+ \sum_{\Gamma\subset\partial S\cap\partial\Omega} h_S^3\,\|g - \nu\cdot\nabla U^n\|_\Gamma^2\Big).
\end{aligned}$$

Here, $[\nabla U^n]_\Gamma$ denotes the jump of the gradient of U^n over an interior edge Γ of the triangulation, h_S is the diameter of mesh element S, and C_τ, C_h are constants. The use of mass lumping generates a few additional terms in the spatial indicator η_S^n.

Now, a quasi-optimal mesh for a given error tolerance is one, where the error is below the given tolerance, while the error indicators are equally distributed over all mesh elements. The adaptive method tries to automatically arrange time step sizes and local mesh

refinement (and coarsening) in order to achieve this goal. In each time step, it starts with the mesh $\mathcal{S}_{n-1}$ from the old time step and computes a discrete solution $\tilde{U}^n \in V_{n-1}$. After computing the error indicators, the time step size is adjusted, when needed, and the mesh is modified by *local* refinements and derefinements of $\mathcal{S}_{n-1}$, where needed. This generates the mesh $\mathcal{S}_n$, where the corresponding discrete system is solved again for $U^n \in V_n$. For slowly (in time) varying solutions, the second solution step can be omitted, speeding up the calculation. To capture fast changing solutions, it may be necessary to iterate the estimate-refine-solve steps in order to reach the prescribed error tolerance.

Application to concrete carbonation

We want to adopt this method for our application of concrete carbonation. In a heuristical way, we can directly setup error indicators $\eta_S^0, \eta_\tau^n, \eta_S^n$ like above, taking into account all equations from the system (9)-(12). Unfortunately, due to the dominant reaction and slow diffusion (i.e., big Thiele modulus), the mathematical derivation will lead to *very* large constants C_τ, C_h, making the error estimate practically unusable, when aiming at the goal to get the overall error below a given tolerance. For this reason, we will use constants $C_\tau = C_h = 1$ for our numerical experiments. A derivation of better estimates and indicators, based on different error norms and/or estimation techniques, requires future work.

5 Numerical Experiments

In order to test the numerical method, results of a carbonation experiment on samples under laboratory conditions have been used. See [10, 11] for a fairly complete description of the test setup. In [11], Thomas and Matthews consider among others the case of a poor OPC concrete with 1 day of curing and w/c=0.7. For the cement in question, a CaO content of about 65% and a density of $300 kg/m^3$ are assumed. To illustrate the calculations, we assume that the concrete structure is exposed to the increased atmospheric concentration of CO_2(g) of an industrial site, which attacks a corner of the structure. In such a setting, CO_2(g) concentration at the exposed boundaries is about 0.0001 kg/m^3 and the relative humidity (in the structure and outside) is about 65%. The rest of the model parameters (for reaction, transport, mass-transfer at water/air interfaces, etc.) are identical with those given in [6]. See the basic geometry in Figure 1. It shows an L-shaped domain with one symmetry boundary edge (on the right). Besides the symmetry edge, the boundary conditions on all other parts of the boundary are the same. Due to the L-shape, we see the reaction behaviour near three convex (outer) and one concave (inner) corners.

Figure 1 shows concentration fields of $CO_2(g)$, $CO_2(aq)$, and $Ca(OH)_2$ from four different times during the simulation. Due to the scaling and the assumption of constant porosity and water fractions, the $Ca(OH)_2$ values shown on the right hand sides correspond to the *local carbonation degree*. Note that after a few days of carbonation, a clear separation between a carbonated zone and an uncarbonated one appears. After such a

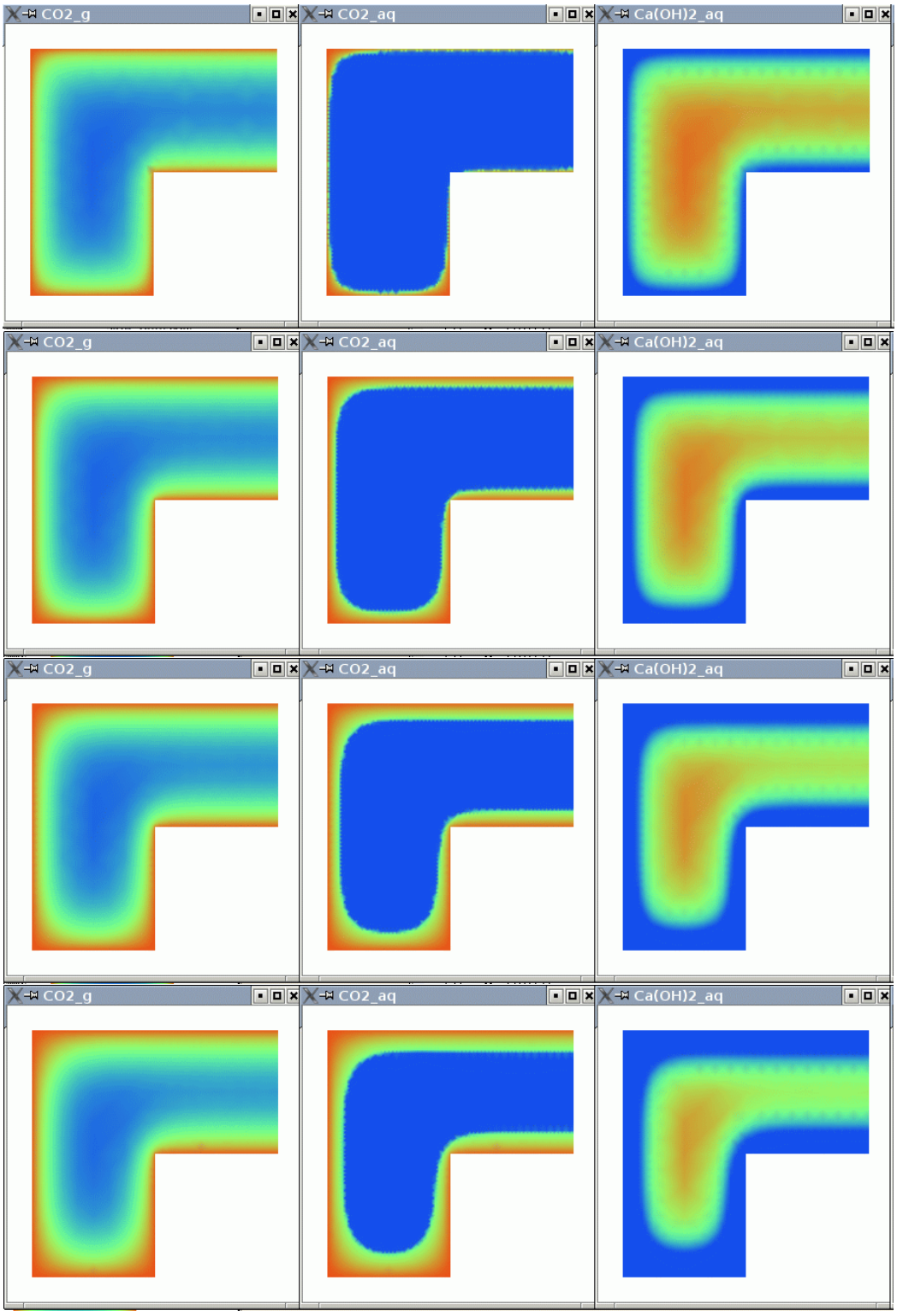

Figure 1: Concentration fields from four different times, showing a clear separation of reactants: $CO_2(g)$, $CO_2(aq)$, and $Ca(OH)_2$, from left to right.

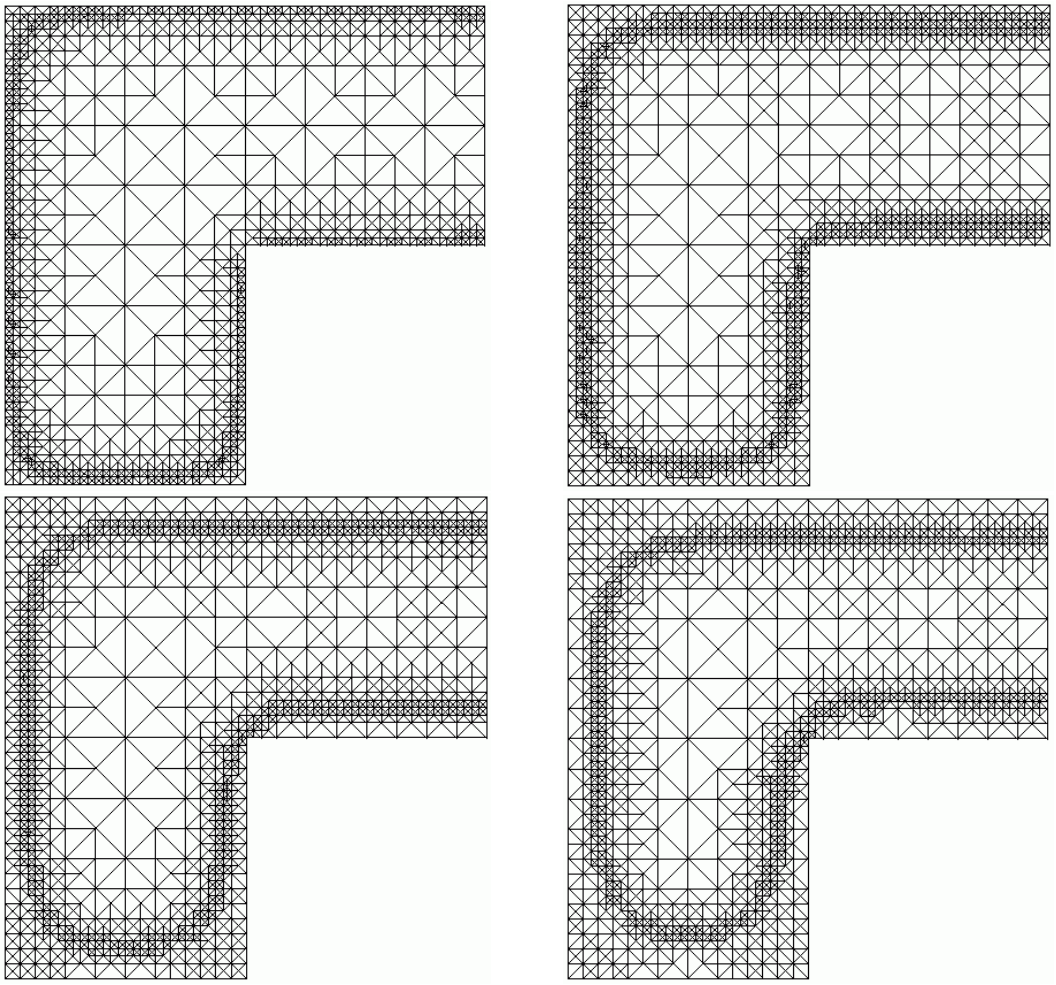

Figure 2: Automatically adapted meshes at four different times, corresponding to concentration fields in Figure 1. After a transient time, an internal reaction layer is formed and progresses into the material. This moving reaction layer is automatically captured by the self-adaptive mesh refinement method.

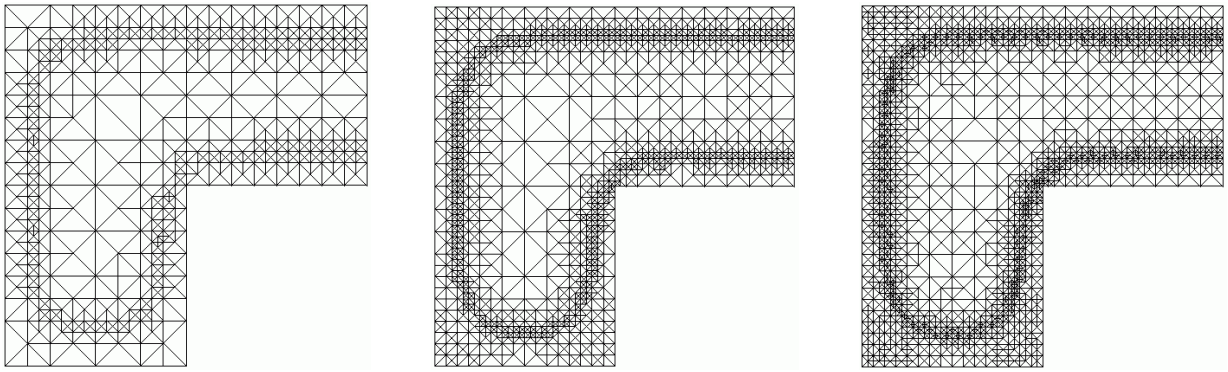

Figure 3: Meshes from three simulations with different refinement tolerances.

transient time, a thin reaction layer (called carbonation front) is formed. Near the convex outer corners, the carbonation front progresses faster than at straight edges, and it moves even slower near the concave inner corner. Since we only look at the first days of carbonation, relatively few moisture is produced by reaction, thus we don't show the moisture concentration. Figure 2 shows corresponding meshes from four different times, with automatic high refinement near the carbonation front. In Figure 3, we show the influence of different refinement criteria on the resulting meshes. Taken at the same time, it shows meshes with same tolerance as in Figure 2 (middle), as well as tolerances chosen 4 times bigger (left) and 4 times smaller (right).

The implementation of the numerical code was done using the adaptive finite element toolbox ALBERTA [9], which is based on simplicial meshes in 1D, 2D, 3D, where mesh elements are intervals, triangles, and tetrahedra. The toolbox does local mesh refinement by bisection of elements. Here, for a 2D simulation, a initially coarse subdivision of the domain into triangles gets successively locally refined, until the local error indicators are small enough. In each time step, the error indicators are computed and the mesh locally adapted (refined or coarsened), when needed.

6 Conclusions

We have demonstrated that self-adaptive finite element methods can provide an appropriate tool for efficient and reliable numerical solution of reaction-diffusion problems where moving internal reaction layers occur, and forecast of chemical attack in concrete structures. Narrow reaction zones can automatically be resolved by the adaptive method.

Although the current method is mainly heuristical, future investigations and studies may lead to customized error estimates and error indicators, giving (mathematically proven) reliable information about the numerical approximation error between exact and computed solution.

Acknowlegments. This work has been partially supported by the Deutsche Forschungsgemeinschaft (DFG) by a grant through the special priority program SPP1122 "Prediction of the Course of Physicochemical Damage Processes Involving Mineral Materials".

References

[1] O. Burkan-Isgor: A Durability Model for Chloride and Carbonation Induced Steel Corrosion in Reinforced Concrete Members. PhD thesis, Department of Civil and Environmental Engineering, Carleton University, Ottawa, Ontario, Canada, 2001.

[2] T. Chaussadent: États de lieux et réflexions sur la carbonatation du beton armé. Technical report, Laboratoire Central de Ponts et Chaussées, Paris, 1999.

[3] K. Eriksson and C. Johnson: Adaptive finite element methods for parabolic problems I: A linear model problem. SIAM J. Numer. Anal. 28 (1991), pp. 43-77.

[4] K. Eriksson and C. Johnson: Adaptive finite element methods for parabolic problems IV: Nonlinear problems. SIAM J. Numer. Anal. 32 (1995), pp. 1729-1749.

[5] J. Kropp: Relations between transport characteristics and durability. In J. Kropp and H. K. Hilsdorf (Eds): Performance Criteria for Concrete Durability, RILEM Report 12, pp. 97-137. E and FN Spon Editions, 1995.

[6] S. A. Meier, M. A. Peter, A. Muntean, and M. Böhm: Modelling and simulation of concrete carbonation with internal layers. Manuskript, ZeTeM Univ. Bremen, 2005.

[7] A. V. Saetta, B. A. Schrefler, and R. V. Vitaliani: 2d model for carbonation and moisture/heat flow in porous materials. Cem. Concr. Res. 25 (1995), pp. 1703-1712.

[8] Robert Sandboge: Adaptive finite element methods for systems of reaction-diffusion equations. Comput. Methods Appl. Mech. Eng. 166 (1998), pp. 309-328.

[9] A. Schmidt and K. G. Siebert: Design of adaptive finite element software: The finite element toolbox ALBERTA. Springer LNCSE Series 42, 2005.

[10] A. Steffens, D. Dinkler, and H. Ahrens: Modeling carbonation for corrosion risk prediction of concrete structures. Cem. Concr. Res. 32 (2002), pp. 935-941.

[11] M. D. A. Thomas and J. D. Matthews: Carbonation of fly ash concrete. Mag. Concr. Res. 44 (1992), pp. 160 ff.